Journal of Physics: Conference Series **554** (2014) 012002 doi:10.1088/1742-6596/554/1/012002

Parameters of the NERA spectrometer for cold and thermal moderators of the IBR-2 pulsed reactor

I Natkaniec[1,2], D Chudoba[1,2], Ł Hetmańczyk[1,3], V Yu Kazimirov[1], J Krawczyk[1,4], I L Sashin[1] and S Zalewski[1,5]

[1]Joint Institute for Nuclear Research, Frank Laboratory of Neutron Physics, Joliot-Curie 6, 141980 Dubna, Russian Federation
[2]Adam Mickiewicz University, Faculty of Physics, Umultowska 85, 61-614 Poznań, Poland
[3]Jagiellonian University, Faculty of Chemistry, Ingardena 3, 30-060 Kraków, Poland
[4]H. Niewodniczański Institute of Nuclear Physics, Polish Academy of Sciences, Radzikowskiego 152, 31-342 Kraków, Poland
[5]Siedlce University of Natural Sciences and Humanities, Institute of Chemistry, 3 Maja 54, 08-110 Siedlce, Poland

E-mail: inat@jinr.ru

Abstract. The inverted geometry time-of-flight spectrometer NERA designed for simultaneous investigation of elastic and inelastic neutron scattering was constructed on a 100 meter long flight path of the IBR-2 reactor at JINR, Dubna, Russia. Spectrometer parameters were optimized for the thermal neutron spectrum of a water moderator at 330 K. Recently, a new type of cold neutron source operating at 30 K was installed in the sector of six horizontal channels. The cold source in combination with the water moderator allows one to effectively use incident neutrons in wide range of wavelengths.

1. Introduction

A 100 meter long flight path on channel no. 7 at the IBR-2 pulsed reactor was constructed in the 1980's for high resolution studies of condensed matter by neutron powder diffraction (NPD), quasielastic (QENS) and inelastic neutron scattering (INS). Two home-made direct Ni-mirror guides with a transversal cross section of the 5 × 16 cm^2, extracted neutron beams 7a and 7b, for instruments located at 103 m and 109 m flight path, respectively. Mirror guides were installed at a distance of 7.5 m from the IBR-2 water comb-like moderator. Beams 7a and 7b crossed at the window of the fast neutrons background chopper located at 5.5 m from the moderator. The background chopper at such geometry of extracted beams was used also as a neutron wavelength selector (λ-chopper) that transmitted the same thermal spectrum for both beams. At 100 m of flight path and a frequency of 5 Hz of IBR-2 pulses, the neutron spectrum must be limited to 7.5 Å to avoid frame overlap. The beam 7a was used for the development of new instruments for effective investigations of crystalline texture and internal stress analyses by the time-of-flight high resolution neutron powder diffraction method. Finally, two modern instruments: SCAT – for texture analysis and EPSILON – for internal stress analysis were constructed [1]. The NERA-PR spectrometer [1,2], located on the beam 7b at a distance of 109.05 m

from the moderator was commissioned in 1991 and operated effectively until the end of 2005, when the IBR-2 reactor was shut down for modernization.

A new type of cold neutron source for the sector of channels 7-11 was constructed during the modernization period 2006-2011 [3]. A cold moderator medium, an organic glass of mesitylene and m-xylene solution was selected as a result of investigations of the structural properties and methyl group dynamics of solid phases of methyl derivatives of benzene [4, 5], which were performed on the NERA-PR spectrometer. The modernization program for spectrometers located on 100 m flight paths of channel no. 7 included the replacement of the old neutron guides and extraction of three independent beams. The three new mirror guides begin after the background chopper window at a distance of 6 m from the moderator. The first 10 m long common vacuum section which contains three mirror guides with direct visibility of moderator is called the 'splitter'. Independent neutron guides (7a1 - EPSILON, 7a2 – SCAT and 7b – NERA) begin at a distance of 16.5 m from the moderator.

In this paper we compare the parameters of the NERA spectrometer before and after the modernization of the IBR-2 pulsed reactor, including the new cold moderator and the replacement of the neutron guides.

2. Modernization of the NERA spectrometer

The layout of the inverted geometry NERA spectrometer is shown in figure 1. The primary spectrometer defines the energies of the incident neutrons and transports the neutron beam from the IBR-2 moderator (2) to the sample position (11) at L_1 = 109.05 m. A new fast neutron background chopper (4) rotates around a horizontal axis and is located in the inner corridor of the IBR-2 reactor shielding at an unchanged distance of 5.5 m from the moderator. The chopper disc has the same diameter of 134 cm, however, the thickness of the TiH_2 layer which removes fast neutrons was doubled to 6.2 cm. The rotating disc window forms the 60° sector free of TiH_2 layer. The present geometry of the extracted beams, which are separated at the background chopper window, makes it impossible to use the λ-chopper mode of the background chopper satisfactorily for all three spectrometers due to different phases.

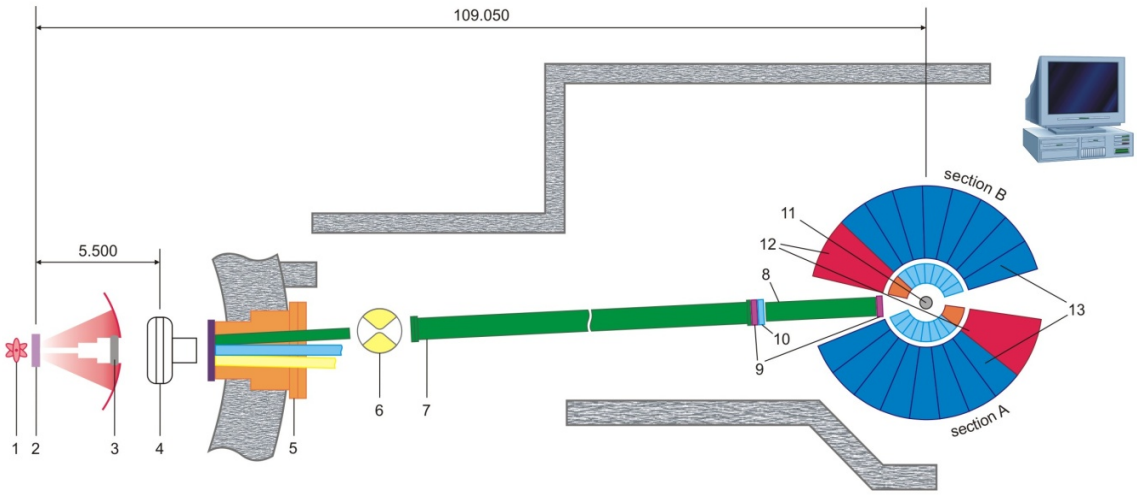

Figure 1. The layout of the NERA spectrometer: 1 – IBR-2 reactor core, 2 – thermal and cold moderators of radial horizontal channels 7-11 and tangential channels 1–9, 3 – beam shutter, 4 – fast neutron background chopper, 5 – common vacuum splitter of three Ni-mirrors neutron guides, 6 – λ-chopper of beam 7b, 7 – vacuum Ni–mirrors guide tube of neutron beam 7b, 8 – vacuum sections of beam 7b, 9 - diaphragms of incident beam, 10 –monitor, 11 – sample position, 12 – NPD sections, 13 – INS and QENS sections.

The splitter (5) transports three neutron beams from the inner corridor to a distance of 16.5 m out of the biological shielding of the reactor. From this place, the neutron beams are transported by independent vacuum Ni-mirror guide tubes (7).

Due to the fact that experiments with cold neutrons up to λ = 14 Å were planned on beams 7a1 and 7a2, a new velocity selector (λ-chopper) was constructed and installed at a flight path distance of L_λ = 26.95 m from moderator. The λ-chopper drum (diameter = 48 cm) rotates in the vertical axis at a frequency of 2.5 Hz, which is half that of the frequency of the IBR-2 pulses. A TOF diagram, transmission function, as well as a general view and rotor window shape are presented in more detail in figure 2.

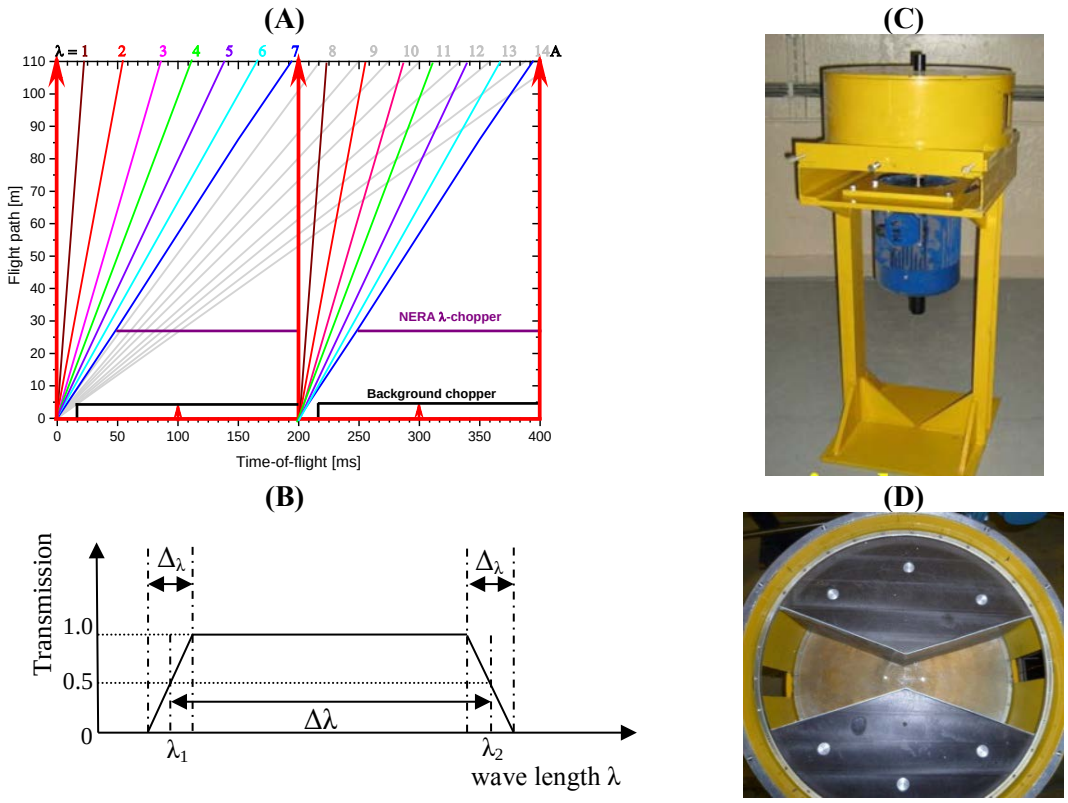

Figure 2. TOF diagram - (A) and transmission function - (B) of the λ-chopper beam 7b, where $\lambda_2 - \lambda_1 = \Delta\lambda$ = 7.1Å, Δ_λ = 0.975Å. General view (C) and the drum rotor (D) of installed λ-chopper.

As part of the modernization, the evacuated Ni-mirror guide tube was replaced. The transversal dimension of the new neutron guides is 5 × 16 cm^2 as it was before. The main part of the 80 m long vacuum guide tube ends 2 m before the sample position. An additional vacuum section 1.5 m long includes a monitor counter and a beam-shaping diaphragm in the incident beam.

The design features of the main part of the NERA spectrometer, which analyses and records the scattered neutrons, are presented in figure 3. The spectrometer consists of two symmetrical sections, A and B. One scattering chamber for NPD and eight chambers for INS and QENS measurements are located in each of them. For NPD measurements neutrons scattered by the sample (1) pass through collimators (3) and are detected with two kinds of detectors: cylindrical He-3 counters (7) without additional collimation, which record NPD spectra at high luminosity, and rectangular He-3 counters (8) positioned after long Soller collimators, which record NPD spectra at a low background level. The NPD spectra are recorded at scattering angles of $30^o \leq 2\theta \leq 70^o$ and $110^o \leq 2\theta \leq 150^o$.

Details of the INS and QENS scattering chambers are presented in figure 3. The neutrons scattered by a sample (1) pass through the common beryllium filter collimators (2), which are cooled by liquid nitrogen. At this temperature beryllium only transmits the neutrons with energy less than 5.25 meV. The INS and QENS spectra are recorded at scattering angles from 20° to 160° in 10° increments.

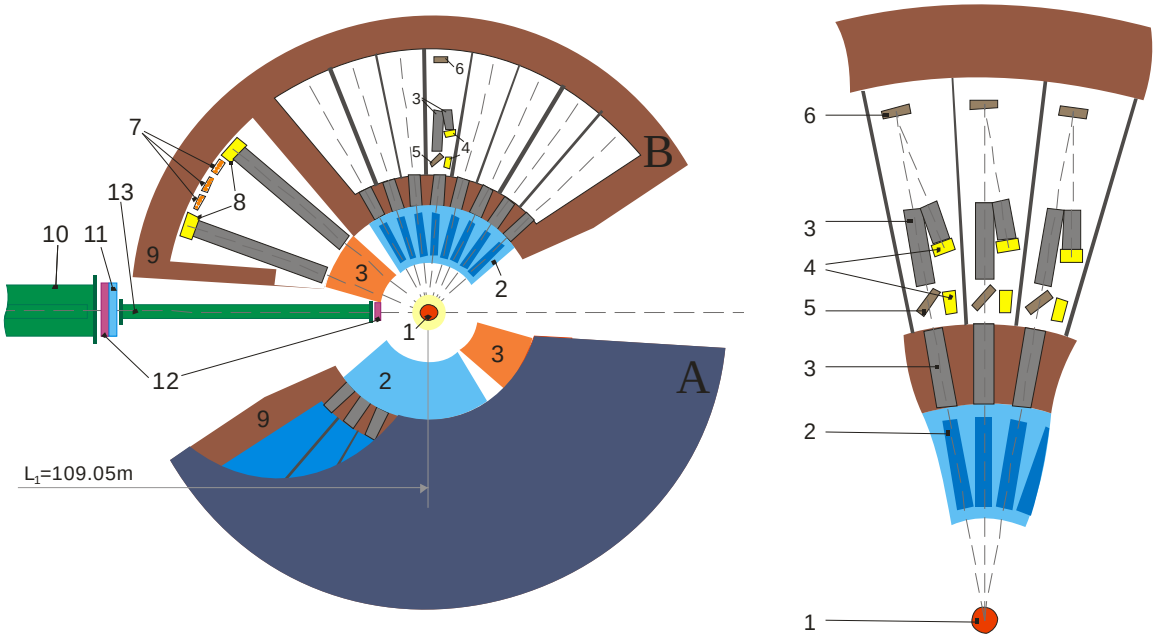

Figure 3. The main part of the NERA spectrometer: 1 - sample, 2 - Be-filters, 3 - collimators, 4 – He-3 detectors (INS and QENS), 5 - PG analysers (INS), 6 - single crystal analysers (QENS), 7 – detectors for high intensity diffraction, 8 – diffraction detectors with a good collimation, 9 - spectrometer shielding, 10 - Ni-coated mirror neutron guide in a vacuum tube, 11 - incident beam monitor, 12 – diaphragms, 13 - vacuum neutron guide.

There are three possible ways to analyse the energy of scattered neutrons with different resolution:
- by using the beryllium filters and detectors located directly behind them. In this case the spectrometer has high luminosity at low energy resolution,
- by using beryllium filters and pyrolytic graphite – PG(002) analysers at the scattering angle $2\Theta = 90^{o}$ before the detectors. This is a main option of spectrometer for measurements of the INS spectra with medium resolution and reasonable intensity,
- by using beryllium filters and crystal analysers (Cu, Al, Zn or PG) at the scattering angle $2\Theta = 174^{o}$. In this case the INS luminosity is very limited but the width of elastic lines (40 - 60 μeV) is suitable for investigations of quasielastic neutron scattering. This mode can be carried out simultaneously with the second one, because the elastic line positions of the crystal analysers at backscattering differ from those of the neutron energies reflected by pyrolytic graphite at $2\Theta = 90^{o}$.

The modernization of the NERA automatic control instruments and TOF analyser electronics, as well as operational and computing software for recording, processing and visualization of experimental data will be the subject of a separate paper.

3. Time of flight incident neutron spectra

A low efficiency gaseous proportional counter filled with a mixture of nitrogen and inert gases is used for monitoring the incident neutron flux on the NERA spectrometer. The time-of-flight (TOF) spectra of incident neutrons measured by the monitor counter are shown in figure 4.

Spectrum A was measured with fully open windows of stationary background and λ-choppers. One can see that it was recorded at a rather high background of overlapping neutrons, which have lost correlation with the reactor pulses and diffused inside the mirror guide. This background can be effectively removed by proper phasing of λ-chopper with the IBR-2 pulses, as it is shown by spectra B and C. At phase F1, which corresponds to spectrum B, the transmission window of λ-chopper shown in figure 2, is fully open at the time of the IBR-2 pulse. The bent mirror guide does not transfer fast and epithermal neutrons up to 16 ms after the reactor pulse, which corresponds to the neutron wavelength of λ = 0.6 Å. Spectrum C, recorded with phase F2 = F1 + 16 ms, corresponds to the optimal transfer without overlapping of the wavelength range λ = (0.6 - 6.6) Å, as was intended in the design of the λ-chopper.

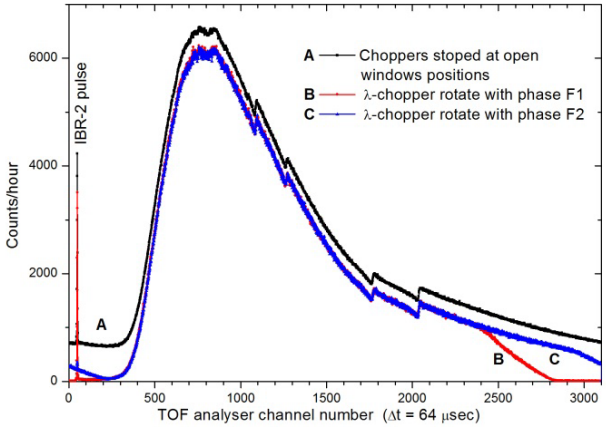

Figure 4. The TOF incident neutrons spectra measured by monitor counter for water moderator (WM) at different phases of the λ-chopper.

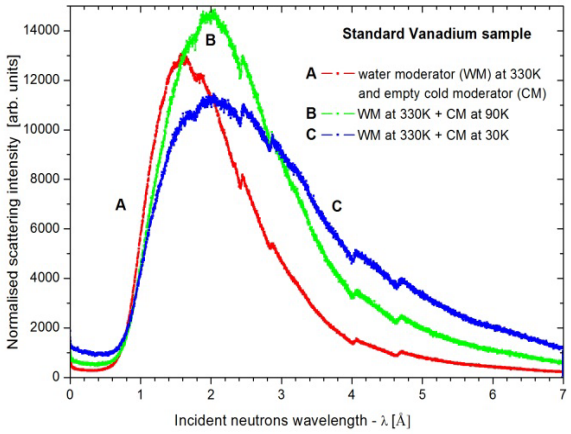

Figure 5. The TOF spectra measured by diffraction detectors after scattering by vanadium sample for water (WM) and cold moderator (CM) at different temperatures.

Incident neutron spectra of the water and cold moderators as measured by the diffraction detectors after scattering from the standard vanadium sample are shown in figure 5. The standard sample was prepared from 100 g of vanadium foil, rolled in a shape of a cylindrical tube 5 cm in diameter and 20 cm high. This sample matches the transversal cross-section of the neutron guide and scatters all incident neutrons at the sample position. Using this standard vanadium sample we can determine the efficiency of the detector system and compare parameters of the NERA spectrometer for a long time period.

The TOF incident neutron spectra measured before and after the reconstruction of the IBR-2 are compared in figure 6 in a wavelength scale. The TOF scale has been transformed into the incident neutron wavelength by using the following relation:

$$\lambda = h/mv \quad \text{or} \quad \lambda[\text{Å}] = 3.956 \times 10^{-3}\, t[\mu\text{s}]/L[\text{m}],$$

where: h is Planck's constant, λ, m and v - are the neutron wavelength, mass and velocity respetively, t - is the time of flight and L – is the average total distance from the IBR-2 moderator to the NERA diffraction detectors. The average total distance L can be calculated from the cut-off edges of the aluminium windows in the path of the neutrons from the moderator to detectors, which are clearly seen in all incident neutron spectra. These edges correspond to the neutron wavelength

λ(hkl) = 2d(hkl) of the corresponding interplanar distances of the Al crystal structure. The calculated average value of L is (110.47 ± 0.1) m. The NPD detectors (He-3 counters, 2 cm thick) are placed at the radius L_{2D} = (1.415 ± 0.01) m from the centre of the sample position. The flight path of the NERA spectrometer calculated in this way has a value equal to $L_1 = L - L_{2D}$ = (109.05 ± 0.05) m.

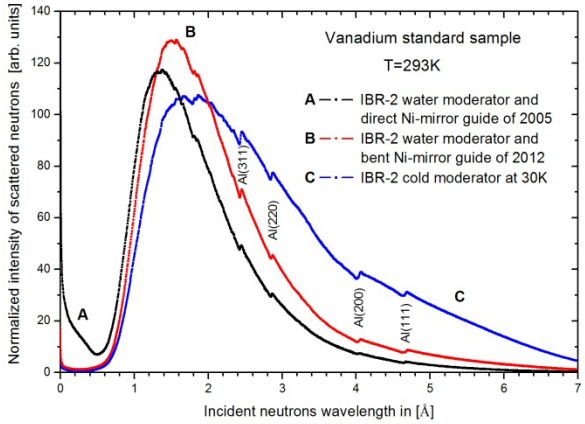

Figure 6. Incident neutrons spectra before and after modernization of the IBR-2 moderator and the Ni-mirror vacuum neutron guides of the beam 7b, normalized to average power of the reactor.

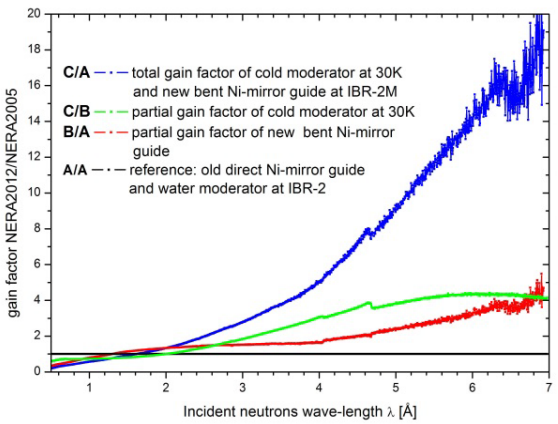

Figure 7. Gain factors versus incident neutron wavelength after the modernization of the IBR-2 moderator and the Ni-mirror neutron guides of the NERA spectrometer.

By comparing the spectra shown in figure 6, one can conclude that the mirror guide 7b has no direct visibility of the IBR-2 moderator, since the epithermal neutrons present in spectrum A are absent in spectra B and C. A direct neutron guide was planned in the modernization project of beam 7b, however, a mistake was made when the splitter was adjusted in optimal way for the neutron beams 7a1 and 7a2. As a result it was not possible to conduct the direct beam 7b to the experimental pavilion and the last 80 m section of the NERA mirror guide had to be slightly bent in order to transport neutrons to the sample position.

The integrated values of spectral distributions shown figure 5 in the range of λ = (0.5 - 6.5) Å have the following ratio relations: B/A = 1.34 and C/A = 1.27. The reference spectrum A corresponds to the water moderator and an empty cold moderator container. Spectra B and C correspond to the fully loaded container of the cold moderator with mesitylene pellets at 90 K and 30 K, respectively. One can see that the integrated neutron flux increases by 34% when the cold moderator container was filled with mesitylene at 90 K. Further cooling of moderator to 30 K, slightly decreases the integrated gain factor to 1.27, because cold neutrons with λ > 6.5 Å are beyond the integration limits.

The integrated values of the spectra shown in figure 6 are in the ratio: B/A = 1.2 and C/A = 1.6. Here the reference spectrum A corresponds to the comb-like water moderator in 2005, the year before the reconstruction of the IBR-2 reactor core. The B and C spectra correspond to the new thermal water moderator and the cold moderator at 30K, respectively. The value 1.2 of the integrated gain factor of the water moderator thermal neutron flux means that the new bent mirror guide transports 20% more neutrons than the old direct mirror guide. The better quality of the new Ni-mirror neutron guide also contributes to the fact that the neutron flux at the sample position from the cold moderator is greater by 60% as compared to the old comb-like water moderator.

The partial and total spectral gain factors versus incident neutron wavelength are shown in figure 7. From the comparison with the reference spectrum of neutrons transported by the old direct mirror guide in 2005, one can see that the partial gain factor of the new bent mirror guide for water moderator becomes grater then one for λ > 1.3 Å, increases twice at λ = 4 Å, and further increases linearly to five

at λ = 7 Å. The partial gain factor of the new cold moderator over the new water moderator becomes greater than one at λ = 2 Å, linearly increases to 4 at λ = 4.7 Å and remains at this value up to λ = 7 Å. The total gain factor of the new cold moderator and Ni-mirror guide in 2012 compared to the old moderator and mirror guide in 2005 becomes greater than one at λ = 1.5 Å and increases up to about 20 at λ = 7 Å.

4. Energy analysis of the scattered neutrons and resolution of the NERA spectrometer

A set of energy analysers of the scattered neutrons consists of polycrystalline beryllium filters cooled to liquid nitrogen temperature and pyrolytic graphite (PG) or single crystal Cu or Zn in front of the detectors. Be-filters eliminate higher order reflections of the basal plane of crystal analysers. The Be-filters can be used as the energy analysers for a high intensity INS mode at low resolution of the spectrometer when the detectors are placed directly after them. Spectral distributions of neutrons scattered by a standard vanadium sample and registered by the helium-3 detectors are shown in figure 8, versus incident neutrons wavelength, and in figure 9, versus final energy scattered neutrons.

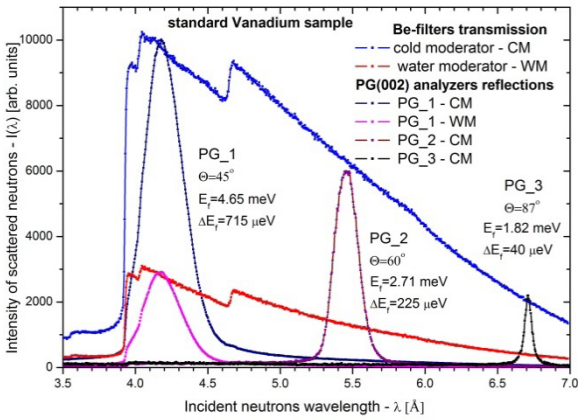

Figure 8. Transmission of the Be-filters and reflections of the PG(002) analyzers at different Bragg angles - Θ.

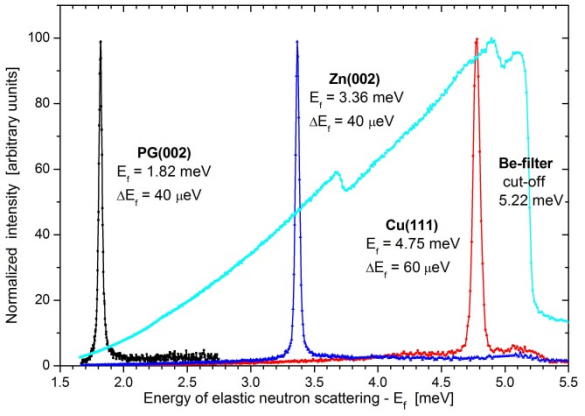

Figure 9. Final energies and FWHM of elastic peaks of different crystal analyzers at nearly back scattering reflection - 2Θ = 174°.

The significant gain of neutron flux in the wavelength range of λ = (4 - 7) Å given by the cold moderator, as shown in figure 7, enables us to use crystal analysers at nearly back scattering for INS and QENS spectra in the high resolution mode of the NERA spectrometer (see figure 9).

The intensity of neutrons $I(t,\varphi,T)$ which were scattered at an angle φ and sample temperature T, and recorded at time t can be expressed as a convolution of the scattering cross section $\sigma(E_i,E_f,\varphi,T)$ with the incident neutron flux $\Phi(E_i)$ and the instrumental resolution $R(E_i, E_f, t_0, t)$

$$\boldsymbol{I(t,\varphi,T)\Delta t = \Delta t \iiint \sigma\left(E_i,E_f,\varphi,T\right)\Phi(E_i)R\left(E_i,E_f,t_0,t\right)dE_i dE_f dt_0} \quad (1)$$

where: Δt is the time interval corresponding to the channel width of the time-of-flight analyser, E_i and E_f are incoming and scattered neutron energies, respectively.

The resolution function of NERA spectrometer can be written as:

$$\boldsymbol{R\left(E_i,E_f,t_0,t\right) = \rho(E_i,t_0)n\left(E_f\right)\delta(t-t_0-t_1-t_2)} \quad (2)$$

$\rho(E_i, t_0)$ is the time distribution of incoming neutrons with the energy E_i leaving the source at time t_0. It can be calculated as a convolution of the fast neutron pulse shape with a function that describes the moderation process of neutrons. The fast neutron pulse shape of the IBR-2 is a Gaussian function with FWHM equal to 215 μs, and the parameters of moderation function for the comb-like water moderator were determined in [6].

$n(E_f)$ is the energy distribution of scattered neutrons, as shown in figures 8 and 9.

$\delta(t-t_0-t_1-t_2)$ gives the condition for registration of neutrons at time t, which left the source at time t_0 with energy E_i and were scattered to energy E_f.

$t_1=\alpha L_1/\sqrt{E_i}$ is the flight time of neutron with energy E_i of the flight path L_1 = 109.05 m.

$t_2=\alpha L_2/\sqrt{E_f}$ is the flight time of the scattered neutron with energy E_f from the sample to detector distance L_2 = 1.015m,

α = 2286.27 is a conversion coefficient of neutron energy to velocity when time is expressed in [μs], flight path in [m] and energy in [meV].

The resolution functions of the different components of inverted geometry spectrometers are presented in more detail in [7].

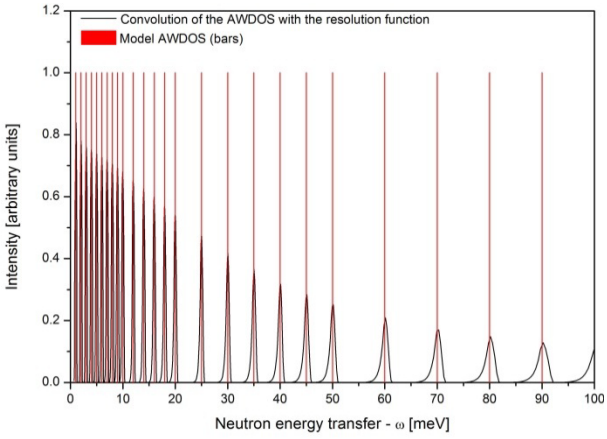

Figure 10. Shape of resolution functions of the NERA spectrometer for PG(002) analyzers reflection at scattering angle 2Θ = 120°, calculated according to eq. (1).

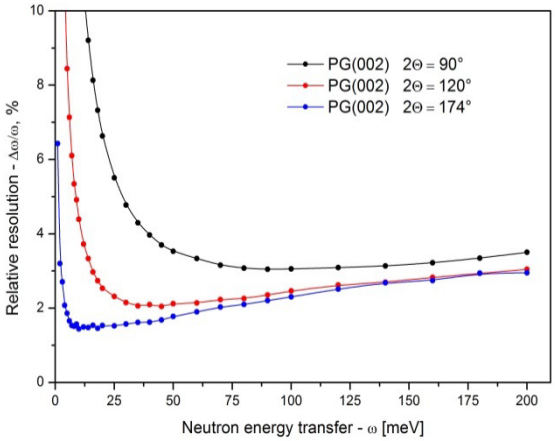

Figure 11. Relative resolution of the INS spectra measured with PG(002) analyzers at different scattering angles 2Θ = 90°, 120° and 174°.

The scattering cross-section for phonon creation process at low temperatures can be written in the incoherent one-phonon scattering approximation in the following way

$$\sigma_1^{inc}(E_i, E_f, \varphi, T) \approx \sqrt{\frac{E_f}{E_i}} \frac{\hbar |Q(E_i,E_f,\varphi)|^2}{\omega} \sum_n \frac{(b_n^{inc})^2}{M_n} \frac{exp(-2W_n)}{1-exp\left(-\frac{\hbar\omega}{k_B T}\right)} G(\omega) \quad (3)$$

where: $Q(E_i,E_f,\varphi)$ is the neutron momentum transfer, $\omega=(E_i-E_f)$ is the neutron energy transfer, b_n^{inc} is the value of the incoherent scattering length, M_n is the mass of the n^{th} atom, $exp(-2W_n)$ is the Debye-Waller factor and $G(\omega)$ is the so-called amplitude weighted phonon or vibrational density of state (AWDOS), defined as:

$$G(\omega) = \sum_j \int d^3q \left[A_j^n(q,\omega)\right]^2 \delta\left[\omega - \omega_j(q)\right] \text{ or } G(\omega) = \sum_j \sum_n \left[A_j^n(\omega)\right]^2 \delta\left(\omega - \omega_j\right) \quad (4)$$

$A_j^n(\omega)$ is the amplitude of displacement of the n^{th} atom in the unit cell at the vibration mode $\omega_j(q)$, j- is an index that runs over all the dispersion curves or internal normal modes and **q** is a reciprocal lattice wave vector in the Brillouin zone.

Computational models, which give frequencies $\omega_j(q)$ and displacement amplitudes $A_j^n(q,\omega)$ of atomic vibrations in the crystal unit cell or in atomic or molecular clusters, allow one to calculate directly the INS TOF spectra in the approximation of one-phonon incoherent scattering process, according to equations (1), (2), (3) and (4).

Assuming the model of the AWDOS functions, in the form of δ-functions at a given energy transfer is as shown in figure 10, one can directly calculate the shape of the resolution function of the NERA spectrometer according to equation (1), by convolution of experimentally determined energy

distribution functions: $\Phi(E_i)$, $\rho(E_i, t_0)$ and $n(E_f)$ at the TOF condition $\delta(t\text{-}t_0\text{-}t_1\text{-}t_2)$. The relative resolution functions of the INS spectra $\Delta\omega/\omega$ versus neutron energy transfer $\omega=E_i-E_f$ are presented in figure 11.

5. Background ratio and luminosity of inelastic scattering and neutron powder diffraction

A standard sample of 10 ml of water in a rectangular 1 × 60 × 160 mm^3 Al sample holder was measured with thermal and cold moderators in order to check the correctness of the transformation of TOF INS spectra into the AWDOS functions G(ω). The background level of an empty sample holder and the cryostat in this case do not exceed several percent of the INS intensity. However, the water sample produces a very high incoherent background at the NPD detectors. The TOF INS spectra of ice, measured at 20 K with PG_1 analysers (2Θ = 90^o) and summed over 15 scattering angles in the range from 20^o to 160^o, are compared in figure 12.

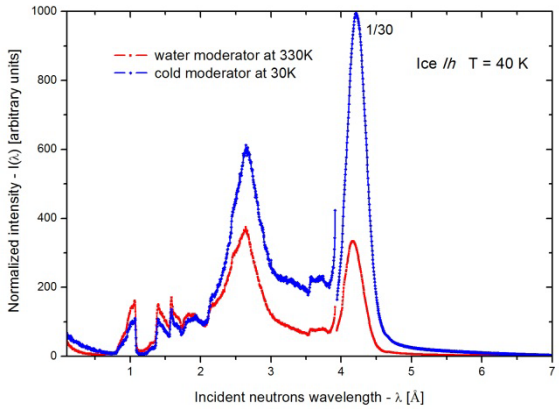

Figure 12. The experimental TOF INS spectra of Ice *1h* measured at T=40 K for thermal and cold moderators of the IBR-2 pulsed reactor.

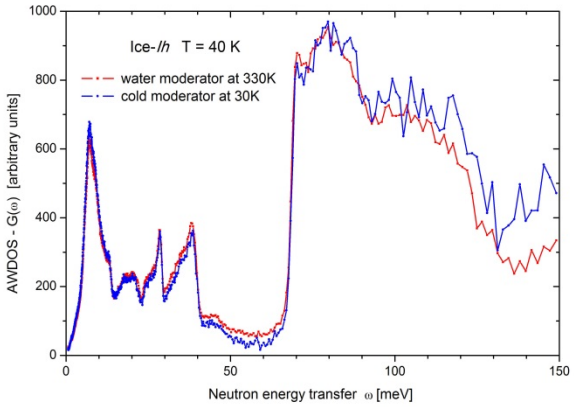

Figure 13. Amplitude-weighted density of phonon states (AWDOS) *G(ω)* of Ice *1h* obtained from the TOF INS spectra from figure 12.

The spectra measured with thermal and cold moderators were normalized to 10 hours measurement time at a constant reactor power and similarly processed background spectra were subtracted. After such normalization we could not obtain consistent *G(ω)* functions of ice for both moderators. The reason was that the incident neutron fluxes of both moderators were normalized to unity at their maxima by the NERA software, while they have the same values only at the wavelength λ = 2 Å (see figure 6). The TOF INS spectra normalized to integrated monitor counts or measurement time do not fulfil this condition for normalization, as well. Additional normalization of the TOF INS spectra of ice to the same value at λ = 2 Å results in almost identical *G(ω)* functions shown in figure 13.

The transformation of the TOF INS spectra to *G(ω)* is done omitting the convolution procedure and using average values of spectral distribution functions written in equations (1) and (2). The IBR-2 pulse shape under this assumption is characterized by $\delta(t - T_0)$, where T_0 is an average delay time between the electronic pulse starting the TOF analyser and the real neutron pulse of the reactor. The average energy of incident neutrons $E_i(i)$, where *i* is the channel number of TOF analyser, is calculated by the relation introduced in section 4:

$E(i)$ [meV] = $(\alpha L_1$[m]$/t_1(i)$ [μsec]$)^2$, where: $t_1(i) = (i - 1/2)\Delta t - T_0 - t_2$.

The final energy of the scattered neutrons E_f depends on the particular crystal analyser used; their spectral distributions and average values are shown in figures 8 and 9.

The intensity of the scattered neutrons in the TOF INS spectra, $I(\lambda)$, normalized to incident neutron spectra, $\Phi(\lambda)$, defines the scattering cross-section. For hydrogen-containing materials the incoherent inelastic scattering of hydrogen atoms dominates the scattering power of other atoms. By assuming

one-phonon incoherent scattering process and using average values of $E(i)$ and E_f one can transform the INS TOF spectra to the generalized density of vibrational states function $G(\omega)$ directly by using equation (3).

The experimental conditions for investigation of materials with low coherent scattering cross-sections can be illustrated by recently measured INS and NPD spectra of graphitized mesoporous carbons (GMCs) and graphene oxide (GO), which are compared with the reference spectra of spectroscopic purity (99.99%) graphite powder (Grs) in figures 14 and 15.

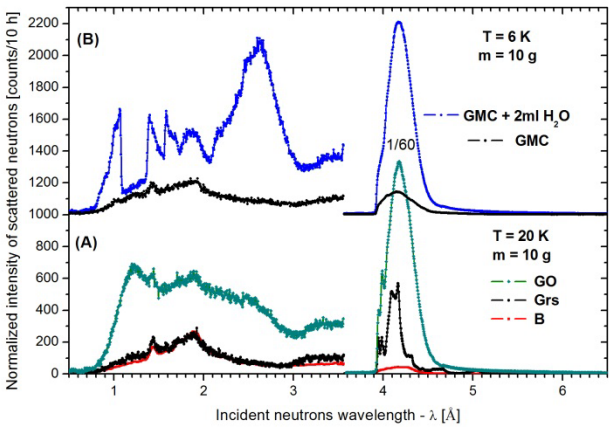

Figure 14. The INS TOF spectra: (A) - empty cryostat – B, spectral graphite – Grs and GO; (B) - GMC and GMC with pores filled by water.

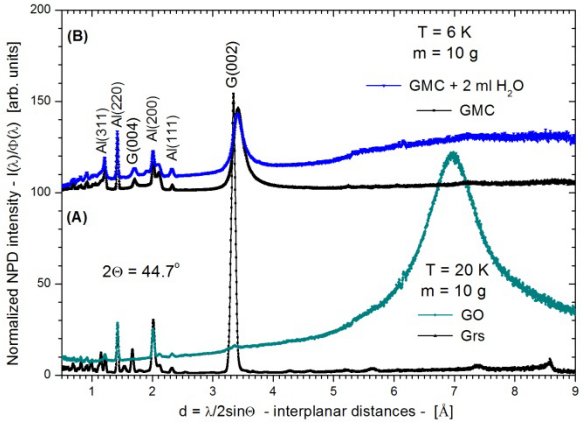

Figure 15. Neutron diffraction patterns: (A) - spectral graphite – Grs and GO, (B) - GMC and GMC with pores filled by water.

GMCs just like spectral graphite (Grs) are almost pure carbon hydrophobic materials, so the 10 gram samples are practically invisible in the INS spectra above the background spectrum (B) of the aluminum cryostat and an empty sample holder. The investigated sample of GMC (Aldrich Product No. 699624) is characterized by an average pore diameter of 14 nm and total pore volume of 0.24 cm^3 $gram^{-1}$. By adding 2 ml of water to 10 grams of GMC in a hermetically sealed container and warming it for several days at 350 K, a powdered sample of GMC with the pores filled with water was obtained. The INS spectra of dry and wet GMC samples are presented in figure 14. As one can expect from the value of average diameter of pores of investigated GMC material, water frozen in the pores of GMS has similar INS spectrum to that of ice *1h* presented in figure 12.

The chemical composition of GO is close to C/O = 2. The GO contains oxygen and hydroxyl functional groups bound to the basal plane of graphene and is a strongly hydrophilic material [8]. The scattering intensity of the INS spectrum of 10 gram GO sample exceeds by several times the background level. By comparing the integral intensity of the INS spectra of GO and GMC filled with water, one can evaluate the hydrogen atom content in the GO sample at the level of about 2 ml of water. The INS spectrum of GO differs significantly from that of ice *1h* and it is the subject of recent studies by INS and computational quantum chemistry DFT methods [9-11].

The NPD spectra shown in figure 15 were recorded for the scattering angle $2\Theta = 44.7^o$ at which interplanar distances can be measured up to 9 Å. The recorded spectra $I(\lambda)$ were normalized to integral counts of the monitor and to the spectral distribution of the incident neutrons $\Phi(\lambda)$. Spectral graphite – Grs along with the GMC samples are clearly seen in the NPD spectra because of the high reflectivity of the (002) graphite plane. The diffraction peaks of Al and Grs correspond to resolution function. Much broader peaks observed for the GMC and GO samples reflects the thickness of graphite or graphene stacks in the investigated nano-carbon materials. A broad diffraction peak at about 7 Å in the GO sample spectrum indicates that the interplanar distance between graphene sheets in graphite oxide

is twice as large as in graphite. This allows water molecules to migrate between of the graphene oxide sheets.

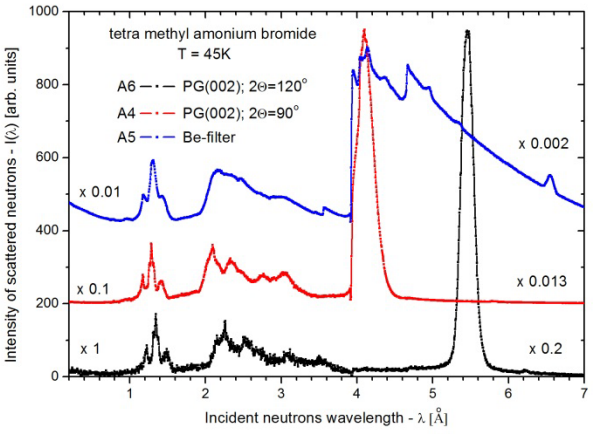

Figure 16. Intensity and resolution of INS TOF spectra measured with different analyzers of neighboring detector chambers at scattering angles 130° (A4), 120° (A5) and 110° (A6).

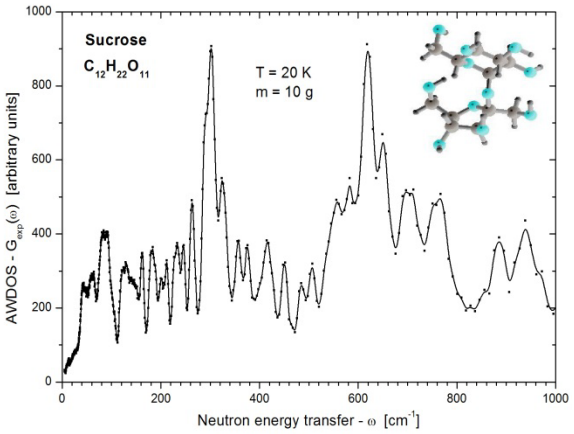

Figure 17. Experimental AWDOS $G_{exp}(\omega)$ function of sucrose chosen for illustration of resolution and luminosity of the NERA in the useful frequency range.

The relationship between the resolution and luminosity of the NERA spectrometer are illustrated in figure 16, by the INS spectra of tetramethyl ammonium bromide measured at 45 K. The scattered intensity of the INS TOF spectra measured at neighboring detector chambers for different energy analysers were normalized to 10 hours measurement time. Taking into consideration the energy window of the analysers used, characterized by the FWHM of final energy distributions: A5 – (Be-filter, ΔE_f = 2.5 meV), A4 – (PG at $\Theta = 45^o$, ΔE_f = 0.715 meV) and A6 – (PG at $\Theta = 60^o$, ΔE_f = 0.225 meV), one can see that the scattered intensity decreases by one order of magnitude when the final energy window narrows by a factor of about three, it means according to the general rule that the luminosity is proportional to the square of the energy window. However, 10 hours measurement time for 10 grams hydrogenous substances seems to be sufficient to record the total spectrum summed over 15 scattering chambers within the resolution window of 0.2 meV. The experimental AWDOS – $G_{exp}(\omega)$ function obtained for sucrose [12] is shown in figure 17 as an illustration of the recent resolution and luminosity of the NERA spectrometer. The frequency range measured with relatively good intensity and resolution of PG analyzers at $\Theta = 45^o$ is limited to 1000 cm^{-1} because the bent neutron guide cuts off neutrons with energies above 150 meV.

The results presented in figures 14-17 were obtained in the context of the user program during the first year of operations of the NERA spectrometer after the modernization.

6. Conclusions

The main objectives of the modernization program of the NERA spectrometer proposed in 2006 were realized and after modernization of the IBR-2 core in 2011 the spectrometer was commissioned in September, 2012. The gain factor (2012/2005) for the water moderator regarding the average thermal neutron flux at the sample position is 1.2, which is not high; however, the spectral distribution of incident neutrons changed significantly. The gain factor (2012/2005) for elastic scattering with the cold moderator in the range of wavelength 1.5 Å < λ < 7 Å increases from 1 to 20, which provides much better conditions for measurements of neutron powder diffraction (NPD) and quasielastic neutron scattering (QENS) spectra in a high resolution mode with near back-scattering crystal analyzers. Unfortunately the transmission of the new bent Ni-mirror guide limits the wavelength of

thermal neutrons to about λ = 0.8 Å; as a result the neutron energy transfer for INS spectra is practicably limited to 120 meV (1000 cm^{-1}).

The mechanical design of the main part of the NERA spectrometer is convenient from the viewpoint of flexibility of replacement and adjustment of the crystal analysers in order to adapt their resolution to the experimental needs. The arrangement of the Be-filters and crystal analysers in the horizontal scattering plane significantly limits the luminosity of the NERA analyser. The horizontal scattering plane determined by the central level of incident and scattered beams does not make it possible to increase the effective area of the crystal analysers over the area of the Be-filters windows. The NERA crystal analyser system could be combined with the high luminosity neutron energy analyser LAGRANGE recently constructed at the ILL [13]. Such a combined system would effectively use neutrons scattered in circular geometry both in and down of the horizontal plane. However, such project seems to be too expensive for realization at the IBR-2 in near future.

The simultaneous measurements of the INS, QENS and NPD spectra with different resolutions of the NERA crystal analyzers give a unique possibility for observing the dynamics and structure of investigated samples, what it is very useful for investigations of organic compounds with rich polymorphism under different thermodynamic conditions.

Acknowledgements

The authors are sincerely grateful to the late Professor J.A. Janik and to Professors A.V. Belushkin, W. Nawrocik and J. Wąsicki, as well as to Doctors D.P. Kozlenko and S.A. Kulikov for their keen interest and support of the modernization project of the NERA spectrometer. We thankfully acknowledge the efforts of those who have assisted in the construction and adjustments of a new Ni-mirror guide and λ-chopper of beam 7b including engineers A.P. Bulkin and V.A. Kudryashov from PINP at Gatchina, engineers A.P. Buzdavin, A.N. Chernikov, A.P. Sirotin and V.V. Zhuravlev and their team of technicians from the Neutron Spectrometers Service Department of FLNP JINR who supported the operation and maintenance of cryogenic, electronic, mechanical and vacuum equipment of the NERA spectrometer.

Grants from the Polish Plenipotentiary in JINR for the modernization project of the NERA spectrometer in 2007-2012 are gratefully acknowledged.

References

[1] http://flnp.jinr.ru, FLNP User Guide.
[2] Natkaniec I, Bragin S I, Brańkowski J and Mayer J 1994 in *Proc. ICANS XII Meeting*, Abingdon 1993, Rutherford Appeton Laboratory Report 94-025, **Vol. I** 89-95.
[3] Ananiev V, Belyakov A, Bulavin M, Kulagin E, Kulikov S, Mukhin K, Petukhova T, Sirotin A, Shabalin D, Shabalin E, Shirokov V, Verhoglyadov A 2014 *Nuclear Instruments and Methods in Physics Research B* **320** 70-74.
[4] Natkaniec I, Hołderna-Natkaniec K and Kalus J 2004 *Physica B* **350** 651-653.
[5] Natkaniec I, Shabalin E, Kulikov S and Hołderna-Natkaniec K 2005 *Proc. ICANS-XVII*, Santa Fe, ed G J Russell, J J Rhyne and B V Maes Los Alamos Report LA-UR-06-3904 **Vol. II** 519-529.
[6] Gundorin A N and Nazarov V M 1980 *Comm. JINR* 3-80-721, Dubna.
[7] Kazimirov V Yu and Natkaniec I 2003 *Comm. JINR* P14—2003-48, Dubna.
[8] Lerf A, He H, Forster M and Klinowski J 1998 *J. Phys. Chem. B* **102** 4477.
[9] Buchsteiner A, Lerf A, Pieper J 2006 *J. Phys. Chem. B* **110** 22328.
[10] Sheka E F, Natkaniec I, Rozhkova N N and Hołderna-Natkaniec K 2014 *JETPletters* **99** 754-759.
[11] Drużbicki K and Natkaniec I, *Chemical Physics Letters* 2014 **600** 106–111.
[12] Szostak M M, Piela K, Hołderna-Natkaniec K, Natkaniec I and Bidzińska E 2014 *Carbohydrate Research* **395** 29–37.
[13] Ivanov A I, Jimenez-Ruiz M and Kulda J 2014 J. Phys. Conf. Ser. in press.